



# MODELING AND SIMULATION OF ISFET USING TCAD TOOL FOR VARIOUS SENSING FILMS

Neel Choksi<sup>a\*</sup>, Dewanshu Sewake<sup>a</sup>, Soumendu Sinha<sup>b, c</sup>, Ravindra Mukhiya<sup>b, c</sup>, Rishi Sharma<sup>b, c</sup>

<sup>a</sup>Birla Institute of Technology and Science, Pilani, Rajasthan 333 031, India

<sup>b</sup>CSIR-Central Electronics Engineering Research Institute (CEERI), Pilani, Rajasthan 333 031, India

<sup>c</sup>Academy of Scientific and Innovative Research (AcSIR), New Delhi-110001, India

\*Email: neelchoksi2809@gmail.com

**Abstract:** Ion-Sensitive Field-Effect Transistor (ISFET) is a popular platform for chemical/biochemical sensing. The simulation of the typical Electrolyte-Insulator-Semiconductor structure using commercial TCAD simulators requires mapping of the chemical reactions taking place at the electrolyte-insulator interface to the Fermi-Dirac equations. This paper presents the modelling of ISFET pH sensor using Silvaco<sup>®</sup> TCAD tool and an analysis of the effect of using different sensing films on the performance of the device has been performed. It is observed that the pH sensitivity of ISFET varies significantly with the sensing film deposited on the gate as well as the thickness of the sensing film. We provide a comparative study for Silicon Nitride, Aluminum Oxide and Silicon Dioxide used as sensing films. Output and transfer characteristics are obtained for these films for various pH values. It is observed that aluminum oxide gives better performance than silicon oxide and silicon nitride. The fabrication process of the device with aluminum oxide as the sensing film has been discussed and the effect of thickness of the film on device performance has been shown.

**Keywords:** Electrolyte Model, ISFET, MOSFET, Silvaco, TCAD.

## 1. INTRODUCTION

Traditional pH sensing mechanisms use glass electrodes that are vulnerable to handling issues and inability to operate at high temperatures etc. These glass electrodes are not suitable for measuring the pH in a nano/microsystems because of difficulties in its miniaturisation. The concept of ISFET (Ion-Sensitive Field-Effect Transistor) was introduced by Dr. P. Bergveld in 1970 which can be microfabricated [1]. It overcomes the difficulties in miniaturisation as in the case of glass electrodes and provides a better medium for pH sensing because of its solid state nature, low production cost, low energy consumption and the possibility of lab-on-a-chip integration [2]. Moreover, this platform can also be utilised for chemical/biochemical sensing with proper functionalization of the gate area [3]. Biosensors based on ISFET technology has its applications in the monitoring of blood, environment, analysis of biological and chemical fluids and laboratory detection [4] [5]. This device is compatible with the existing CMOS technology, which is attractive for batch production of sensors along with signal conditioning circuit.

ISFET is based on the concept of MOSFET (Metal Oxide Field-Effect Transistor). In the structure of ISFET, a pH sensing film replaces the metal gate of MOSFET. This film is in direct contact with the electrolyte and is used for detecting the activity of ions in the analyte. The current flowing through the channel of the transistor is modulated by the ion concentration in the electrolyte [6]. The sensitivity of the device depends upon the gate area dimensions as well as the sensing film. The sensing layer of the ISFET is an area of interest for the researchers and they have examined different types of insulators such as

Aluminum Oxide ( $\text{Al}_2\text{O}_3$ ), Silicon Dioxide ( $\text{SiO}_2$ ), Tantalum Pentoxide ( $\text{Ta}_2\text{O}_5$ ) and Silicon Nitride ( $\text{Si}_3\text{N}_4$ ) and various other dielectrics as sensing films [3]. In this paper, we provide a comparison of the effect of using different sensing films, namely, silicon dioxide ( $\text{SiO}_2$ ), aluminum oxide ( $\text{Al}_2\text{O}_3$ ) and silicon nitride ( $\text{Si}_3\text{N}_4$ ) on the sensitivity of ISFET based pH sensor. We also show the effect of thickness of sensing film on the device performance.

The simulations are carried out using the platform provided by Silvaco TCAD. Commercially available TCAD tools cannot model the chemical reactions taking place at the electrolyte-insulator interface. The typical Electrolyte-Insulator-Semiconductor structure has been modeled in this work by mapping the behaviour of cations and anions in the electrolyte region governed by Poisson-Boltzmann equation to holes and electrons as described by Fermi-Dirac distribution.

In the next section, we discuss the electrolyte model developed to simulate ISFET using Silvaco Athena<sup>TM</sup>. The next section discusses the fabrication process of the device. Further, the transfer and output characteristics of ISFET using different sensing films has been discussed and the effect of film thickness on device performance has been shown.

## 2. MODEL FORMULATION

The drain current for both MOSFET and ISFET are given by same expressions in non-saturated region shown by equation (1) [1]

$$I_D = \frac{\mu_n C_{ox} W}{L} \left[ (V_{GS} - V_T) V_{DS} - \frac{1}{2} V_{DS}^2 \right] \quad (1)$$

Here  $\mu_n$  is the mobility of electrons in the inverted channel when we assume n-channel transistor,  $C_{ox}$  is the capacitance per unit area of the gate and  $W$  and  $L$  indicate the channel width and length of ISFET respectively.

The threshold voltage in ISFET is different from MOSFET because the channel inversion in ISFET occurs due to the potential applied using reference electrode as well as the interface charges between the sensing film and electrolyte. Hence, the flat band voltage expression shown in equation 2 includes the effect of the reference electrodes indicated by the term  $E_{ref}$  which is the reference electrode potential with respect to the vacuum.

$$V_{FB} = E_{ref} - \psi_o + \chi^{sol} - \frac{\phi_{Si}}{q} - \frac{Q_{ss} + Q_{ox}}{C_{ox}} \quad (2)$$

Here in equation (2), the surface potential is indicated by  $\psi_o$  represents surface potential i.e. the potential drop across the bulk of the solution and sensing film,  $\chi^{sol}$  is the surface dipole potential of the electrolytic solution, which is a constant. This is due to the result of chemical reaction, which is regulated by dissociation oxide surface groups. Thus, the resulting threshold voltage expression for an ISFET is given by equation (3)

$$V_T = E_{ref} - \psi_o + \chi^{sol} - \frac{\phi_{Si}}{q} - \frac{Q_{ss} + Q_{ox} + Q_B}{C_{ox}} + 2\phi_F \quad (3)$$

From the above expression indicating threshold voltage, it is observed that all the terms are constant in nature, except  $\psi_o$ . The surface potential variation makes the ISFET sensitive to the pH of electrolyte, which controls the dissociation of the surface oxide groups.

Here, the ISFET is modelled using the electrolyte model [7]. The similarity between the equations for holes and electrons in the semiconductor material and the cations and anions present in equilibrium in the electrolyte solution is exploited [8]. Thus a monovalent electrolyte [8] with a dielectric constant equivalent to that of water and bandgap=1.5eV [9] can be modelled as a semiconductor with a density of states given by:

$$N_C = N_V = \begin{cases} 10^{-3} * N_{av} (c_0 + c_{H_B}) & pH \leq 7 \\ 10^{-3} * N_{av} (c_0 + 10^{-14}/c_{H_B}) & pH > 7 \end{cases} \quad [8]$$

Here  $N_c$  and  $N_v$  are expressed in  $cm^{-3}$ ,  $N_{av}$  is the Avogadro's number,  $c_0$  is molar concentration of the salt ions expressed in *mol/lit* in the solution, and  $c_{H_B}$  indicates the concentration of hydrogen ion solution when normalized to

1M [8]. So for  $pH_B = 4$  and  $c_0 = 1mM$ , the density of states  $N_C$  and  $N_V$  are  $6.6253 \times 10^{-17} cm^{-3}$ . The total concentrations of negative and positive ions are equal and hence we can define bulk electrolyte as the region having constant potential and net a charge of the electrolyte as zero [8]. The total concentrations of negative and positive charges are represented by  $n$  and  $p$  respectively.

$$n \cong N_C e^{-\frac{E_C - E_f}{kT}}$$

$$p \cong N_V e^{-\frac{E_f - E_V}{kT}}$$

Fig. 1 shows a typical MOSFET cross section and Fig. 2 shows the ISFET device along with a reference electrode. The reference electrode is made up of gold for the purpose of simulation and fabrication in Athena.

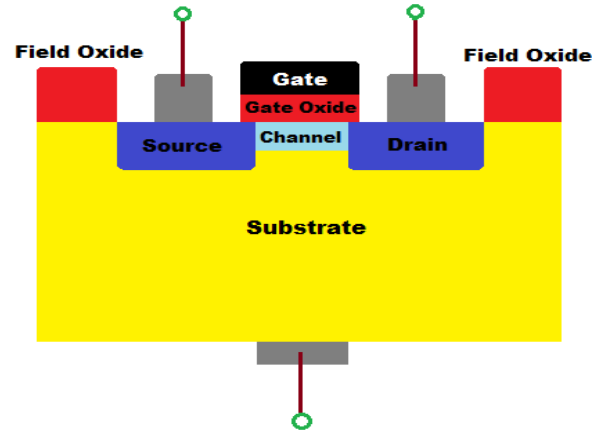


Figure 1. Structure of MOSFET (Not drawn to scale)

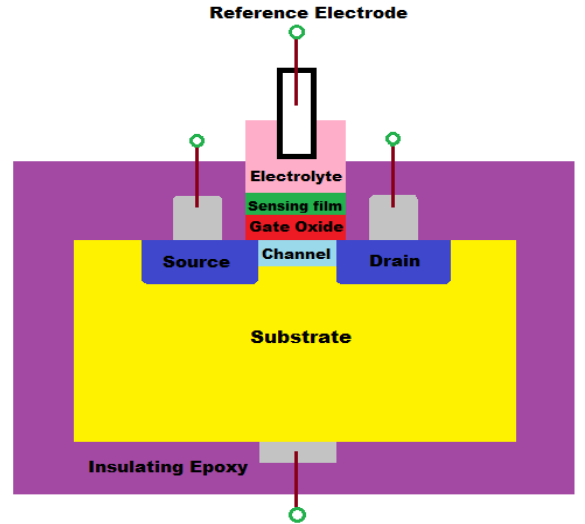


Figure 2. Structure of ISFET (Not drawn to scale)

### 3. FABRICATION PROCESS

In this section, the fabrication process flow for ISFET has been discussed. A 4-inch p-type silicon wafer having a sheet resistivity of 10-20  $\Omega$ -cm has been used. In the first step of the process, silicon dioxide was thermally grown with a thickness of 1  $\mu m$  (Fig. 3.(a)). This step was followed by the patterning of grown oxide for the formation of source and

drain regions with the help of photolithography process (Fig. 3. (b)). The exposed regions were etched out (Fig. 3. (c)). Then, doping of the source and drain regions created in the previous step was carried out by the diffusion of phosphorous atoms followed by the drive-in process (Fig. 3. (d)). Then, the oxide in the gate region was removed. In the next step, aluminum oxide is deposited using reactive sputtering, which is used as the sensing film. Its thickness was kept 1000 Å (Fig. 3. (e), Fig. 3. (f) and Fig. 3. (g)). In the next step, the contacts from source and drain regions were taken out by lithography process. Al<sub>2</sub>O<sub>3</sub> film and oxide layer on the source and drain regions are etched away for this purpose. Then, aluminum metal is sputtered on the wafer which has a thickness of 1 μm. This is further patterned to take out electrical contacts from the device fabricated (Fig. 3. (h), Fig. 3. (i) and Fig. 3. (j)). Annealing of the entire wafer is performed to improve the sensing film characteristics as well as to get better adhesion of aluminum along with the oxide [10]. The entire chip is then insulated from the environment by epoxy resin except for the gate region. It is the gate region which comes in direct contact with the electrolyte solution [11].

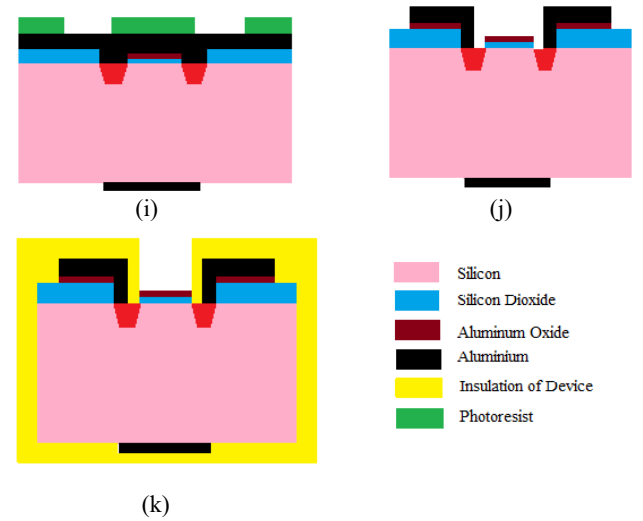
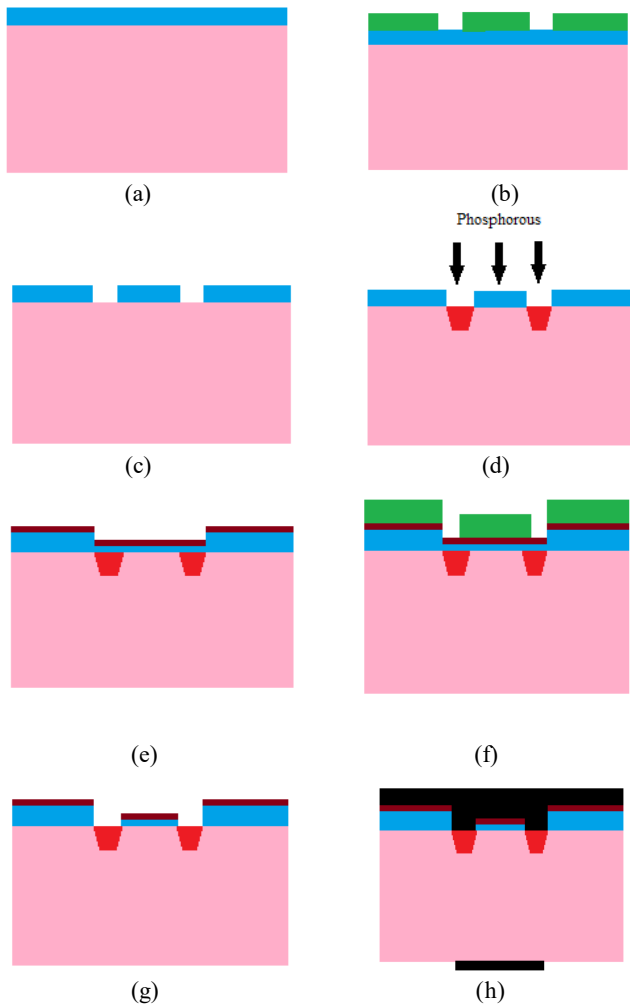


Figure 3. Steps implemented for fabrication of ISFET.

#### 4. SENSITIVITY ANALYSIS

##### 4.1 EFFECT OF SENSING FILM MATERIAL ON SENSITIVITY

The simulation of the transfer and output characteristics of ISFET device was performed using Silvaco Atlas<sup>TM</sup>. For simulation purpose, the semiconductor material for electrolyte region was chosen to be Germanium and its properties were modeled as described in Table – I.

Table I: Parameters for electrolyte region

| Material            | Germanium          |
|---------------------|--------------------|
| Type                | Semiconductor      |
| Dielectric Constant | 80                 |
| Bandgap (eV)        | 1.5                |
| Electron Affinity   | 3.9                |
| Sheet Resistance    | 2.14881 ohm/square |

The structure of ISFET is simulated for different sensing films, SiO<sub>2</sub>, Si<sub>3</sub>N<sub>4</sub> and Al<sub>2</sub>O<sub>3</sub>. The pH of the electrolyte was implemented according to the electrolyte model defined in the second section. The results were simulated for pH values: 3, 7 and 10. For the purpose of simulation, the reference electrode is made up of gold. The structure of ISFET and doping profile simulated in Athena for aluminum oxide as sensing film is shown in Fig. 4 and Fig. 5. Here the thickness of SiO<sub>2</sub> is 50 nm and Al<sub>2</sub>O<sub>3</sub> is 80 nm, and the channel length is 20 μm.

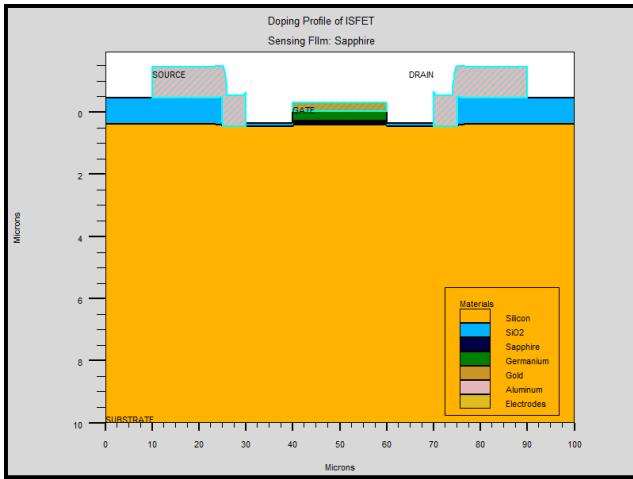


Figure 4. The structure of ISFET with  $\text{Al}_2\text{O}_3$  sensing film built using Athena.

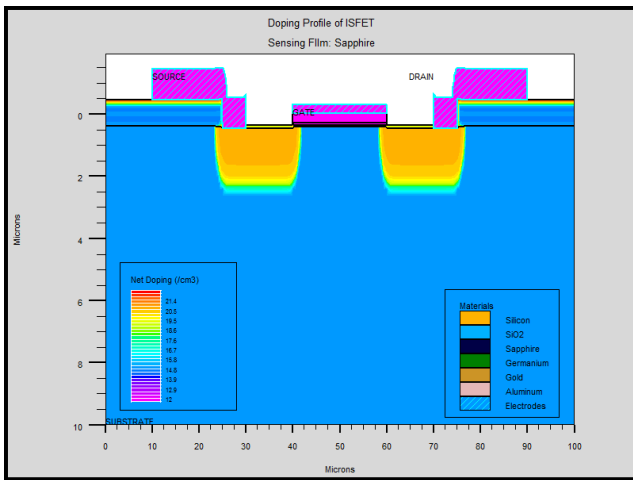


Figure 5. Doping profile for ISFET with  $\text{Al}_2\text{O}_3$  as the sensing film.

Comparison of the  $I_d$  vs  $V_{GS}$  characteristics is shown in the below results for  $\text{SiO}_2$ ,  $\text{Si}_3\text{N}_4$  and  $\text{Al}_2\text{O}_3$  sensing films for pH values of 3 (Fig. 6), 7 (Fig. 7) and 10 (Fig. 8) respectively. For all simulations, the voltage  $V_{GS}$  i.e. the voltage between the gate and the source terminal is varied from 0 to 3V keeping  $V_{DS}$  (Voltage between drain and source terminal is kept fixed) at 0.5V, with the source and bulk terminals grounded.

This transfer characteristics were analysed and the sensitivity was obtained for different sensing films, as summarized in Table-II. It is observed that as pH value of the electrolyte decreases, the value of drain to source current increases, which is in accordance to the behaviour of the drain current in non-saturation as described in equation 1.

$\text{Al}_2\text{O}_3$  based ISFET has better sensitivity than  $\text{SiO}_2$  and  $\text{Si}_3\text{N}_4$  based ISFETs. The calculated sensitivity of ISFET with Aluminum Oxide sensing film is 59.172 mV/pH, which is very near to the Nernstian limit of 59.2 mV/pH. The  $I_d$  vs  $V_{GS}$  characteristics for  $\text{Al}_2\text{O}_3$  based ISFET is shown for pH values 3, 7 and 10 in Fig. 9.

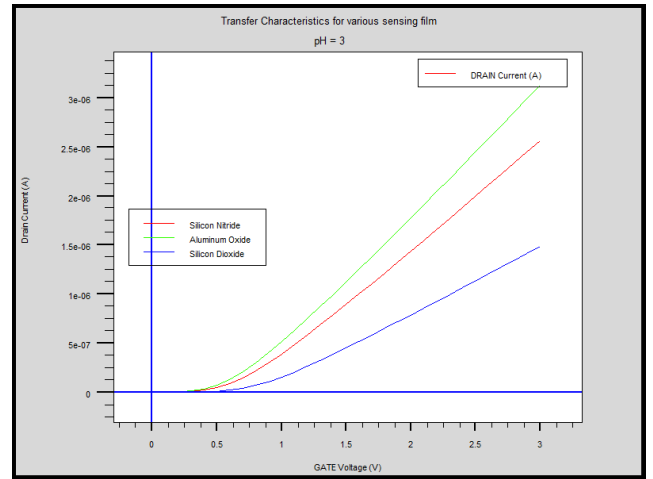


Figure 6. Transfer characteristics for various sensing films at pH value = 3 for the electrolyte.

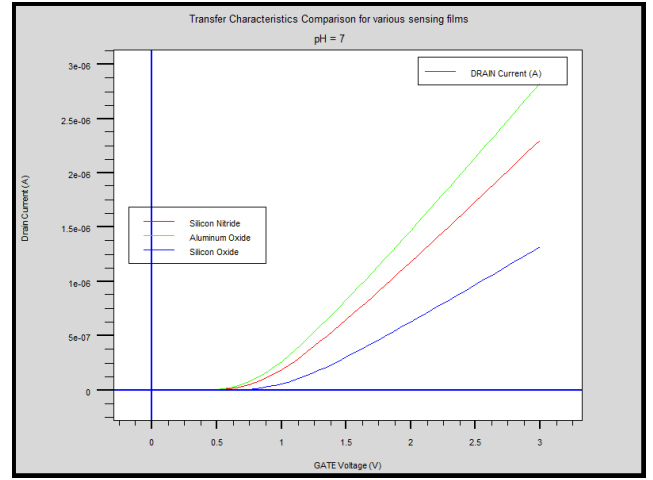


Figure 7. Transfer characteristics for various sensing films at pH value = 7 for the electrolyte.

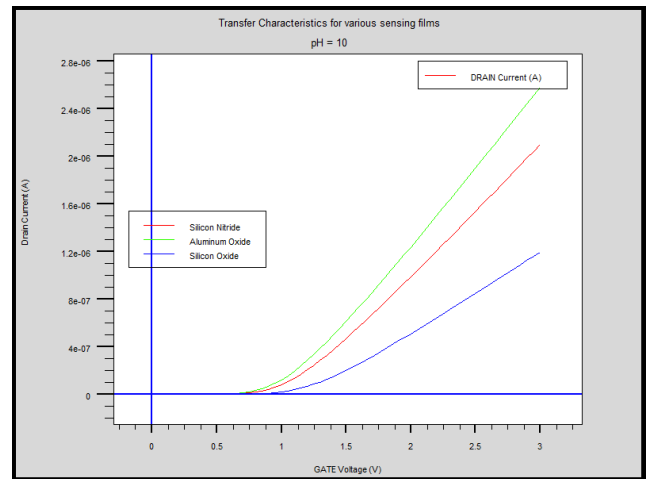


Figure 8. Transfer characteristics for various sensing films at pH value = 10 for the electrolyte.

Table – II: Comparison of sensitivity of different sensing films

| Sensing Film                                | Sensitivity (mV/pH) |
|---|---------------------|
| Aluminum Oxide ( $\text{Al}_2\text{O}_3$ )  | 59.172              |
| Silicon Nitride ( $\text{Si}_3\text{N}_4$ ) | 57.143              |
| Silicon Dioxide ( $\text{SiO}_2$ )          | 54.6                |

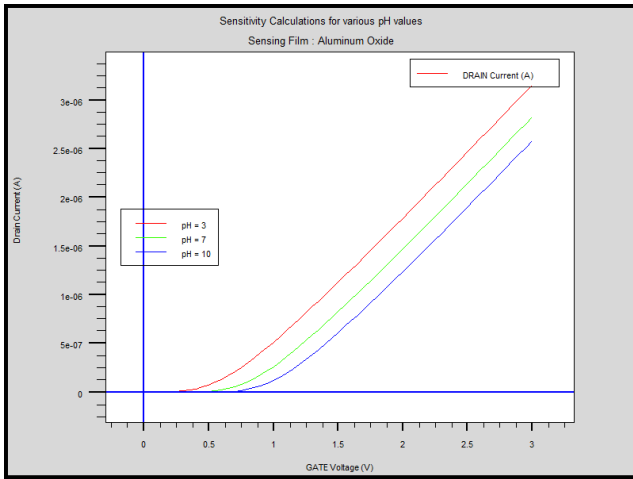


Figure 9. Transfer characteristics for pH = 3, 7 and 10 for  $Al_2O_3$  sensing film.

Fig. 10 gives a comparison of the threshold voltages obtained for various sensing films. It is observed from Fig. 10 that threshold voltage is different for different films and in the case of the  $Al_2O_3$  film, the threshold voltage is least.

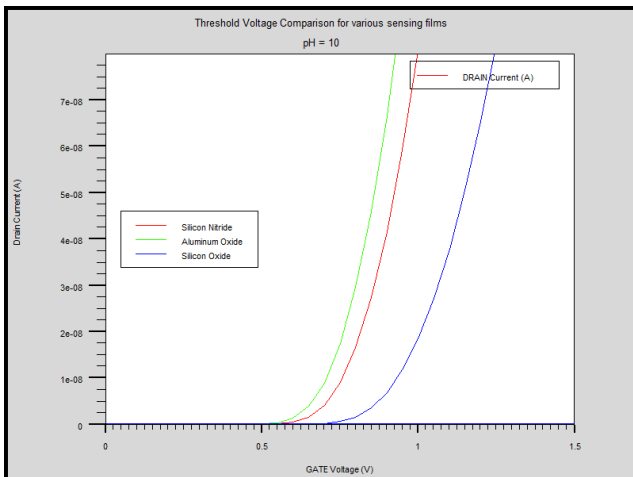


Figure 10. Threshold voltage comparison for various sensing films.

The output characteristics of the  $Al_2O_3$  based ISFET are shown in Fig. 11 for pH = 3. Here, the drain voltage is varied from 0 to 3V for different values of the gate voltage and with the source and bulk terminals grounded.

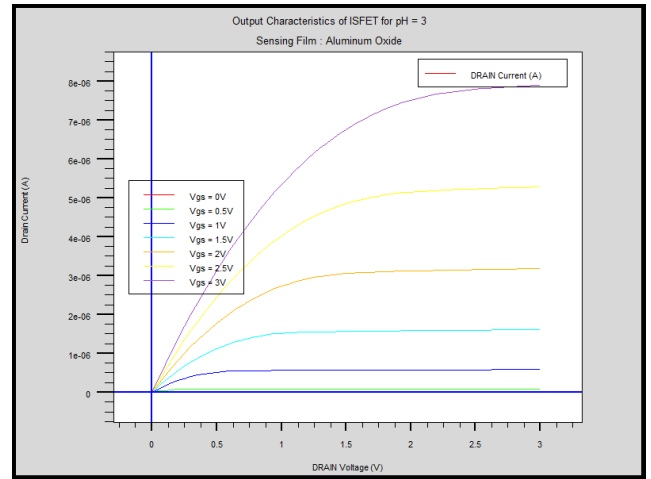


Figure 11. Output characteristics of ISFET for Aluminum Oxide film and pH = 3.

#### 4.2 EFFECT OF THICKNESS OF SENSING FILM ON SENSITIVITY

The other parameter which affects the sensitivity of ISFET is the thickness of sensing film. A comparison is shown in transfer characteristics for film thickness: 50 nm, 100 nm, 150 nm and 200 nm for pH values 3, 7 and 10, as shown in Fig. 12, Fig. 13 and Fig. 14 respectively.

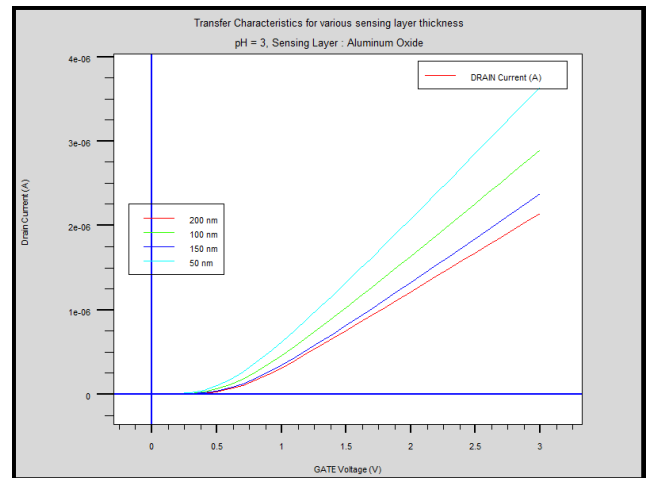


Figure 12. Comparison of sensitivity for various thickness of Aluminum Oxide film when pH = 3.

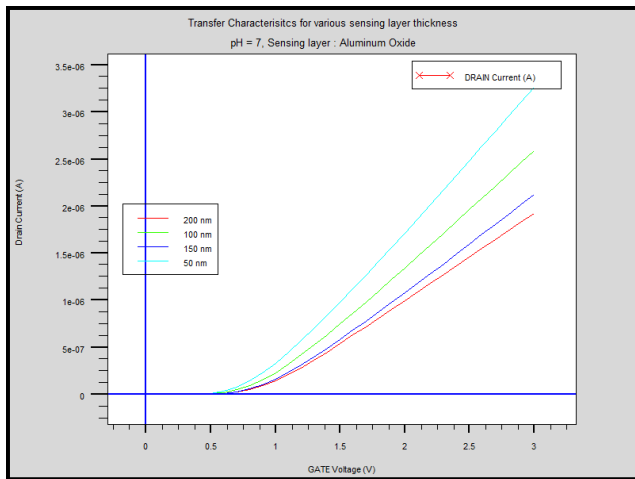


Figure 13. Comparison of sensitivity for various thickness of Aluminum Oxide film when pH = 7.

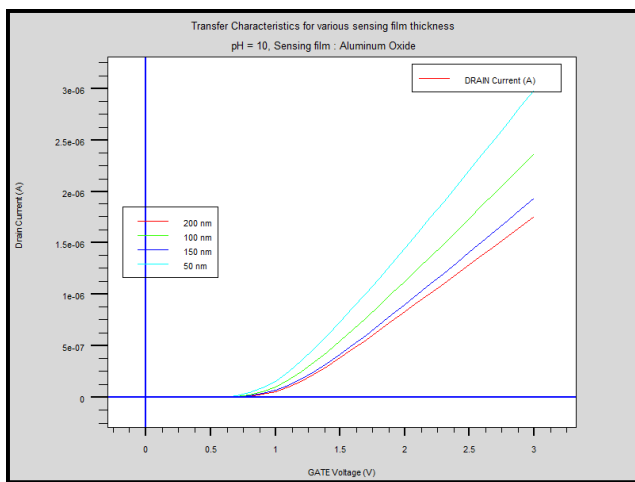


Figure 14. Comparison of sensitivity for various thickness of Aluminum Oxide film when pH = 10.

It can be analysed from Fig. 12, 13 and 14 that for all pH values, maximum sensitivity is obtained for minimum thickness (here 50 nm) of the sensing film.

In Fig. 15 we provide an analysis of change in sensitivity of device for pH=7 and pH=10 when thickness of Aluminum oxide film is changed from 50 nm to 150 nm.

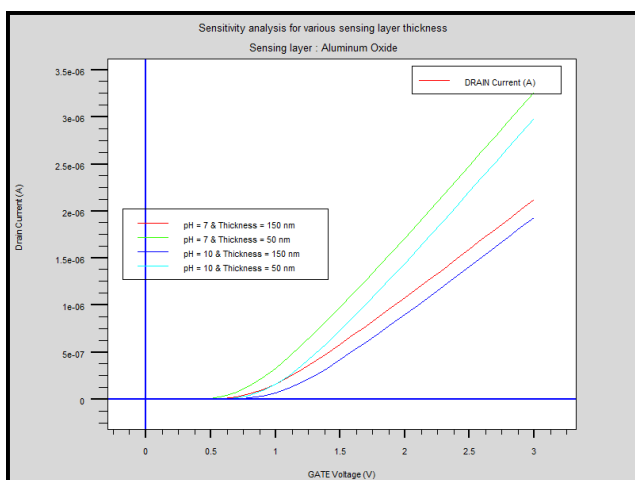


Figure 15: Comparison of sensitivity for different film thickness

It can be observed that for thickness =50 nm we have higher sensitivity of 59.184 mV/pH than for thickness =150 nm for which sensitivity comes out to be 58.91 mV/pH.

## CONCLUSION

In this paper, we have provided a comparative analysis of the effect of different sensing films on the performance of ISFET device. The device is modeled using electrolyte model implemented in Silvaco TCAD tool. The parameters for ISFET were taken in accordance to the ISFET and MOSFET fabricated at the institute laboratory. The simulated sensitivity of Al<sub>2</sub>O<sub>3</sub> based ISFET is 59.172 mV/pH, which is close to the Nernstian limit. Al<sub>2</sub>O<sub>3</sub> films based ISFETs provided better sensitivity than the ones based on SiO<sub>2</sub> and Si<sub>3</sub>N<sub>4</sub> sensing films. The threshold voltage also showed variations upon changing of sensing films for a fixed value of pH. This is due to variation in electrochemical parameters such as density on surface sites and dissociation constants. The sensitivity showed variations upon changing the thickness of the sensing film. Lesser the thickness of the sensing film, higher would be the sensitivity of the device.

## ACKNOWLEDGEMENTS

The authors would like to acknowledge Director, CSIR-Central Electronics Engineering Research Institute for his valuable support. They would also like to thank Director, Birla Institute of Technology and Science, Pilani for his constant support for the work. They are very grateful to all the scientists and technical officers at MEMS & Microsensors Group, CSIR-CEERI, Pilani for their constant support and motivation. This work is financially supported by CSIR, New Delhi, India through project PSC-0201: MicroSenSys (SUPRA Institutional Project).

## REFERENCES

- [1] P. Bergveld, "ISFET, theory and practice.," in IEEE sensor conference, Toronto, 2003.
- [2] P. Bergveld, "Thirty years of ISFETOLOGY: What happened in the past and what may happen in the next 30 years.," sensors and actuators b: chemical, vol. 88, no. 1, pp. 1-20, 2003.
- [3] W. Shinwari, M. M. Jamal Deen and D. Landh, "Study of the electrolyte-insulator-semiconductor field effect," microelectronics reliability, vol. 47, no. 12, pp. 2025-2057, 2007.
- [4] M. Baylav, Ion-Sensitive Field Effect Transistor (ISFET) for MEMS Multisensory Chips at RIT. Diss., ROCHESTER INSTITUTE OF TECHNOLOGY, 2010.
- [5] B. Palan, "Design of low noise pH-ISFET microsensors"PhD Dissertation, 2002.
- [6] L. Bousse, N. F. De Rooij and P. Bergveld, "Operation of chemically sensitive field-effect sensors as a function of the insulator-electrolyte,"

electron devices, IEEE transactions, vol. 30, no. 10, pp. 1263-1270, 1983.

- [7] F. Pittino, P. Palestri, P. Scarbolo, D. Esseni, and L. Selmi, "Models for the use of commercial TCAD in the analysis of silicon-based integrated biosensors," *solid-state electron.*, vol. 98, pp. 63-69, 2014.
- [8] A. Bandiziol, P. Palestri, F. Pittino, D. Esseni and L. Selmi, "A TCAD-Based Methodology to Model the Site-Binding Charge at ISFET/Electrolyte Interfaces," *IEEE transactions on electron devices*, vol. 62, no. 10, OCTOBER 2015.
- [9] D. Welch, S. Shah, S. Ozev and J. Blain Christem, "Experimental and Simulated Cycling of ISFET Electric Fields for Drift Reset," *IEEE electron device letters*, vol. 34, no. 3, March 2013.
- [10] S. Sinha, R. Rathore, A. Sharma, R. Mukhiya and R. Sharma, "Simulation, fabrication and characterization of Dual-Gate MOSFET test structures," in *2nd international symposium on physics and technology of sensors (ISPTS)*, 2015.
- [11] S. Sinha, R. Rathore, A. Sharma, R. Mukhiya, R. Sharma and V. Khanna, "Modeling and Simulation Of ISFET Microsensor for Different Sensing Films," in *ISSS international conference on smart materials, structures and systems*, Bangalore, 2014.